Corneal Aberrations before and after Small-Incision Cataract Surgery

Antonio Guirao,[1] *Jaime Tejedor,*[2] *and Pablo Artal*[3]

Purpose. To study the effect of small-incision cataract surgery on the optical aberrations of the cornea.

Methods. Corneal topography was measured before and after cataract surgery on 70 eyes of 70 patients. Monofocal foldable IOLs were implanted after phacoemulsification through a clear-cornea, 3.5-mm incision without suture. Corneal aberrations, up to the fifth order and 6-mm pupil, were calculated by ray-tracing from the corneal topography. Pre- and postoperative aberrations were compared in each patient and the optical changes induced by surgery investigated.

Results. The root mean square of the wave aberration slightly increased on average after surgery (pre, 0.65 ± 0.46 μm; post, 0.85 ± 0.63 μm). Most aberration terms were similar, averaged across the 70 patients, before and after surgery (spherical aberration: pre, 0.32 ± 0.12 μm, and post, 0.34 ± 0.19 μm; astigmatism: pre, 0.9 ± 0.8 D, and post, 1.1 ± 1.0 D; coma: pre, 0.27 ± 0.18 μm, and post, 0.32 ± 0.33 μm). However, in each patient, there were changes after surgery in the magnitude (either increasing or decreasing) and/or orientation of aberrations. The mean induced astigmatism was −1.0 ± 0.9 D at the orientation of the surgical meridian. Induced trefoil also showed a predominant pattern at this direction. Patients with nasal incisions experienced larger changes.

Conclusions. Small-incision surgery does not systematically degrade the optical quality of the anterior corneal surface. However, it introduces changes in some aberrations, especially in nonrotationally symmetric terms such as astigmatism, coma, and trefoil. The incision site plays a main role in the corneal changes after surgery. (*Invest Ophthalmol Vis Sci.* 2004;45:4312–4319) DOI:10.1167/iovs.04-0693

Today, the implantation of intraocular lenses (IOLs) is a successful procedure for cataracts and aphakia. However, due to the advancements in the field of ophthalmic wavefront sensing during the past few years, new questions and challenges have arisen that require additional study. The quality of the retinal image is mostly limited by the aberrations of the eye. The eye is a complex structure, and each of its components contributes differently to final optical performance. Thus, the study of individual contributions to ocular aberrations has become of great importance for both basic science and clinical applications. The aberrations of the complete eye can be measured currently by using different types of wavefront sensors, or aberrometers.[1–4] The aberrations introduced by the anterior corneal surface can be computed from data obtained by corneal topography.[5] In addition, the combined use of both corneal and ocular aberrations allows the estimation of the aberrations of the crystalline lens.[6–8] In particular, the possibility of measuring the aberrations of the cornea becomes relevant in cataract surgery. Degraded optical quality of the cornea after surgery would limit the performance of the eye with an implanted IOL. Thus, a major concern is to know the possible changes in the corneal optics induced by surgery. It has been shown that an increase in astigmatism may be common after cataract surgery.[9–13] In addition, we have found that the optical performance of the cornea is similar or slightly worse in patients with implanted IOLs,[14] with a small percentage of patients presenting corneal aberrations larger than the average in normal eyes. These conclusions were based on the comparison of corneal aberrations in a group of patients with IOLs after extracapsular cataract extraction in comparison with a group of normal subjects of similar age. A direct comparison in each patient of the corneal aberrations before and after phacoemulsification surgery has not been undertaken.

A related issue in cataract surgery has been the study of how the optics of IOLs combines with the eye's aberrations to produce the final retinal image. It has been shown that typical IOLs, which are manufactured to meet high optical quality standards,[15–18] produce a relatively low retinal image quality.[19] We suggested that the reason could be that conventional IOLs are inadequate for compensating for the aberrations of the cornea.[14] That work inspired a new design of IOLs that compensates for the spherical aberration of the cornea and leads to a partial compensation, similar to the balance that occurs in young subjects between the cornea and the natural lens.[7–8] For these new IOLs to be effective in improving retinal image quality, the optics of the cornea must remain relatively unchanged after surgery.

In this context, the purposes of this work were to study the aberrations of the anterior surface of the cornea in a large population of patients, before and after small-incision cataract surgery, and to investigate the changes in corneal optics induced by the surgery. This information may provide better understanding of the optical performance of eyes implanted with IOLs and can be valuable to look for improvements in the incision procedures in case the surgery produced significant changes in the cornea.

Methods

Patients

Seventy eyes of 70 different patients with cataract were investigated. Ages ranged from 32 to 89 years (mean age, 70 ± 12 years). All clinical examinations and surgery were conducted at the Anterior Segment Division of Ramón y Cajal Hospital (Madrid, Spain). Surgeries were completed between 1999 and 2002 in all patients by the same surgeon (JT). Practices and research adhered to the tenets of the Declaration of

From [1]Departamento de Física, Universidad de Murcia, Murcia, Spain; [2]Departamento de Oftalmología, Hospital Ramón y Cajal, Madrid, Spain; and [3]Laboratorio de Óptica, Departamento de Física, Universidad de Murcia, Murcia, Spain.

Supported by Ministerio de Ciencia y Tecnología Grant BFM2001-0391 (PA).

Submitted for publication June 14, 2004; revised July 23, 2004; accepted August 3, 2004.

Disclosure: **A. Guirao**, None; **J. Tejedor**, None; **P. Artal**, None

The publication costs of this article were defrayed in part by page charge payment. This article must therefore be marked "*advertisement*" in accordance with 18 U.S.C. §1734 solely to indicate this fact.

Corresponding author: Antonio Guirao, Departamento de Física, Universidad de Murcia, Campus de Espinardo (Edificio C), 30071 Murcia, Spain; aguirao@um.es.

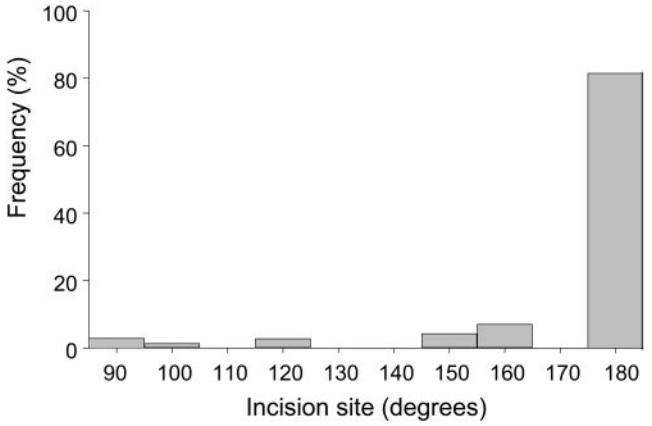

FIGURE 1. Distribution of the incision site in the population of 70 patients studied.

Helsinki. Informed consent was obtained from the subjects after explanation of the nature and possible consequences of the procedures.

Clinical examination data recorded included corrected and uncorrected visual acuity, refraction, manual keratometry, intraocular pressure, and biomicroscopic anterior and posterior segment evaluation. All these tests were performed within 5 days before surgery and at 2 weeks, and between 4 and 6 months after surgery. The preoperative evaluation included biometry and IOL calculation. Videokeratoscopy (Eyemap EH-290; Alcon, Fort Worth, TX) was performed only at the preoperative and 4- to 6-month postoperative follow-up visit. Mean axial length was 23.6 ± 2.1 mm. Mean power of the implanted IOLs was 20 ± 5 D. Mean best corrected decimal visual acuity after surgery was 0.8 ± 0.3. Postsurgical spherical errors ranged from −2.5 to 4.5 D (mean, 0.5 ± 1 D).

Surgical Procedure

Surgery was performed with eyes under topical anesthesia or retrobulbar block. A three-step corneo-corneal incision (2.8 mm blade) was used in all cases. After introduction of viscoelastic material into the anterior chamber, a 5-mm capsulorrhexis was made, followed by hydrodissection, the stop-and-chop phacoemulsification technique, aspiration of cortical masses, and introduction of Acrysof MA60BM (Alcon) or CeeOn edge 911A (Pharmacia & Upjohn Co., Pickerington, OH) foldable IOLs. The corneal incision was enlarged to 3.5 mm to implant the IOL and was not sutured.

The position of the incision was chosen according to a surgical plan for a right-handed surgeon. The criteria for the studied corneas were:

Meridian with the largest curvature at 90 ± 20°: (1) superior incision if ocular astigmatism is 1.5 D or higher or (2) temporal incision for both right and left eyes if ocular astigmatism is lower than 1.5 D.

Meridian with the largest curvature at 180 ± 20°: temporal incision for right eyes and nasal incision for left eyes.

There was no case of oblique astigmatism in the population studied.

Figure 1 shows a histogram with the percentage of patients who had the incision site at each angle. Most patients had the incision at 180°.

Corneal Topography

Corneal topography was measured (EH-290 EyeMap; Alcon). This is a 23-ring Placido-based system that makes a radial sampling of 0.2 mm and a meridional sampling of 10°. The inner ring has a radius of 0.2 mm. This sample density is sufficient for the study of aberrations up to the fifth order for a 6-mm diameter pupil. Sagittal elevations, measured with respect to a reference plane tangential to the corneal vertex, were exported from the topographer as a tabular ASCII file and preprocessed to be used later to calculate aberrations.

The accuracy of the system has been studied by using calibrated testing surfaces.[20] It has been shown that the system is reliable for radial distances up to 3 mm, which is the pupil radius we used for analyzing the aberrations. We tested the reproducibility by comparing four different topographic measurements in the same eye of a patient. Figure 2 shows the mean value and the experimental error of each aberration coefficient, calculated by averaging the four aberration maps obtained from the four different topographies. Also shown is the correlation between the aberration coefficients for the different measurements taken in the same eye. The experimental error due to reproducibility is approximately 0.1 μm for astigmatism, coma, and trefoil coefficients. For spherical aberration the error is much lower: approximately 0.02 μm. The error of the root mean square (RMS), accounting for all the aberrations, is also approximately 0.1 μm. These results are similar to those obtained with others systems[5] and indicate that reproducibility was reasonably good.

The protocol for alignment and focusing the eye was as follows:

1. The patient fixates a small red light in the center of a mire pattern and the operator aligns the eye.
2. The system has autoalignment (centering in the *x*- and *y*-axes with respect to the corneal vertex) and autofocus (positioning in the *z*-axis) mechanisms to enhance manual positioning.
3. Alignment is checked by superimposing a semitransparent topography map on the photokeratoscopy image.
4. The system displays an isometric map, in which the power of the points in each ring are plotted against their axes, as if the rings had been straightened out. Distortion of these profiles may indicate inaccurate alignment.

If positioning was inadequate after these steps, the measurement was discarded and a new topographic map made. Using this protocol, we found high reproducibility when taking multiple measurements, as mentioned in the previous paragraph, and so a single image was finally recorded for processing.

Topography was performed in each patient at the preoperative and 4- to 6-month postoperative follow-up visits.

Corneal Aberrations

We calculated the aberrations produced by the anterior surface of the cornea from the data provided by the corneal topographer.[5] From the elevations at each sampled point, characterized by polar coordinates (r,θ) in the pupil plane, we calculated the corneal wavefront aberration

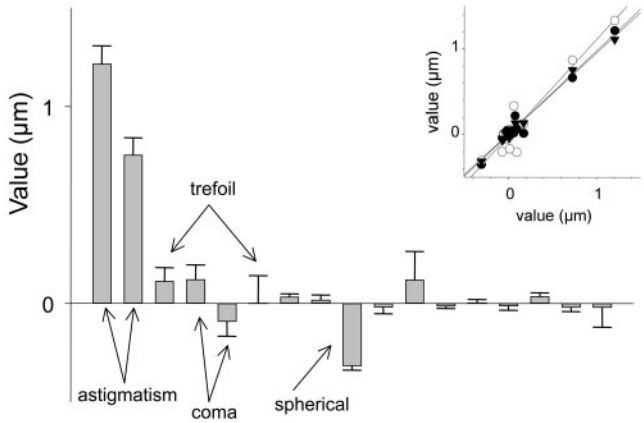

FIGURE 2. Mean value and error bars of each aberration coefficient calculated by averaging four aberration maps obtained from four different topographies in the same eye. *Inset*: correlation between the aberration coefficients for the four different measurements.

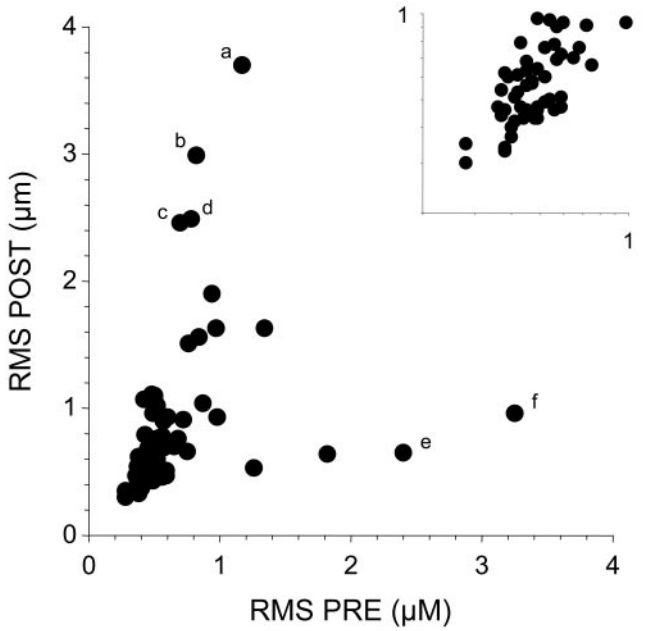

FIGURE 3. RMS of the wave aberration for every cornea before and after surgery. *Inset* is in logarithmic scale between 0.2 and 1 μm.

(WA) as the difference between the optical path lengths of the principal ray passing through the corneal vertex and a marginal ray passing through the point (r,θ)

$$WA(r,\theta) = n's' - n'd' - nz, \quad (1)$$

where n and n' are the refractive indices for the air and the cornea, z is the corneal elevation at the point (r,θ), s' is the distance from the vertex to the image point, and d' is the distance from the point (r,θ) to the image point.

The corneal aberrations were obtained for a pupil 6 mm in diameter. We considered an artificial pupil centered at the corneal vertex. In many cases, the natural pupil is decentered with respect to the vertex. This decentering must be taken into account if, for example, one compares the aberrations of the cornea and those of the complete eye measured by a wavefront sensor that centers with respect to the natural pupil. This consideration was not necessary, however, in the present study. We systematically centered in relation to the vertex, the correct method to use in determining changes in the same eye between two situations.

We obtained the wave aberration up to the fifth order and expressed it as a weighted sum of the first 21 Zernike polynomials, Z_n^m

$$WA(r,\theta) = \sum_{\substack{n=0 \\ m=-n,n}}^{n=5} c_n^m \cdot Z_n^m(r,\theta). \quad (2)$$

Each Zernike coefficient c_n^m corresponds to an individual aberration. For example, $c_2^{\pm 2}$ represents astigmatism; $c_3^{\pm 1}$, coma; $c_3^{\pm 3}$, trefoil (also called secondary, or triangular, astigmatism); and c_4^0, spherical aberration.

The coefficients c_2^{+2} and c_2^{-2} represent the refractive errors along the horizontal meridian and an oblique meridian at 45°, respectively. We calculated the astigmatism in diopters with the equation[5,21]

$$astigmatism = -\frac{1}{r_0^2} 4\sqrt{6}\sqrt{(c_2^{-2})^2 + (c_2^{+2})^2}, \quad (3)$$

where r_0 is the pupil radius (3 mm). The axis of the astigmatism (orientation of the meridian with the lowest curvature) in degrees was calculated as

$$axis = \frac{1}{2}\arctan(c_2^{-2}/c_2^{+2}). \quad (4)$$

The higher order aberrations were quantified by means of the RMS of the wave aberration

$$\text{RMS} = \sqrt{\sum_i (c_i)^2}, \quad (5)$$

with i excluding astigmatism and defocus.

Pre- and postoperative corneal aberrations were obtained in each patient. We performed regression analyses to seek correlations between pre- and postoperative aberrations. We used the two-sample paired *t*-test to determine whether the pre- and postoperative values differed from each other in a significant way. Our data are paired because there is a one-to-one correspondence between the values in the two samples. In most cases, the assumptions of the *t*-test were not met. These assumptions were that differences between samples would be normally distributed (which was examined by the χ^2 test) and that the variances of the two samples would be equal. Although the *t*-test works well with large samples, even if its assumptions are not met, we also used the nonparametric Wilcoxon test. We also investigated the change in the total aberrations separately in two subgroups of patients, depending on the position of the incision: nasal (left eyes, near 180°), or temporal (right eyes, near 180°).

The changes between aberrations before and after surgery were studied by means of "induced aberrations." We calculated these induced aberrations as the difference between post- and presurgical values for every aberration term

TABLE 1. Mean ± SD of Aberrations and a Two-Sample Comparison

			P	
	Pre	**Post**	**Paired *t*-Test**	**Wilcoxon Test**
RMS (μm)	0.65 ± 0.46	0.85 ± 0.63	0.016*	0.005*
Temporal	0.64 ± 0.53	0.68 ± 0.29	0.600	0.470
Nasal	0.66 ± 0.42	0.99 ± 0.80	0.030*	0.050*
Astigmatism (D)	0.90 ± 0.80	1.10 ± 1.00	0.044*	0.091
Coma (μm)	0.27 ± 0.18	0.30 ± 0.26	0.245	0.663
Trefoil (μm)	0.31 ± 0.35	0.54 ± 0.49	0.001*	0.000*
Spherical aberration (μm)	0.32 ± 0.12	0.34 ± 0.19	0.207	0.722

* $P < 0.05$, significantly different with a confidence interval of 95%.

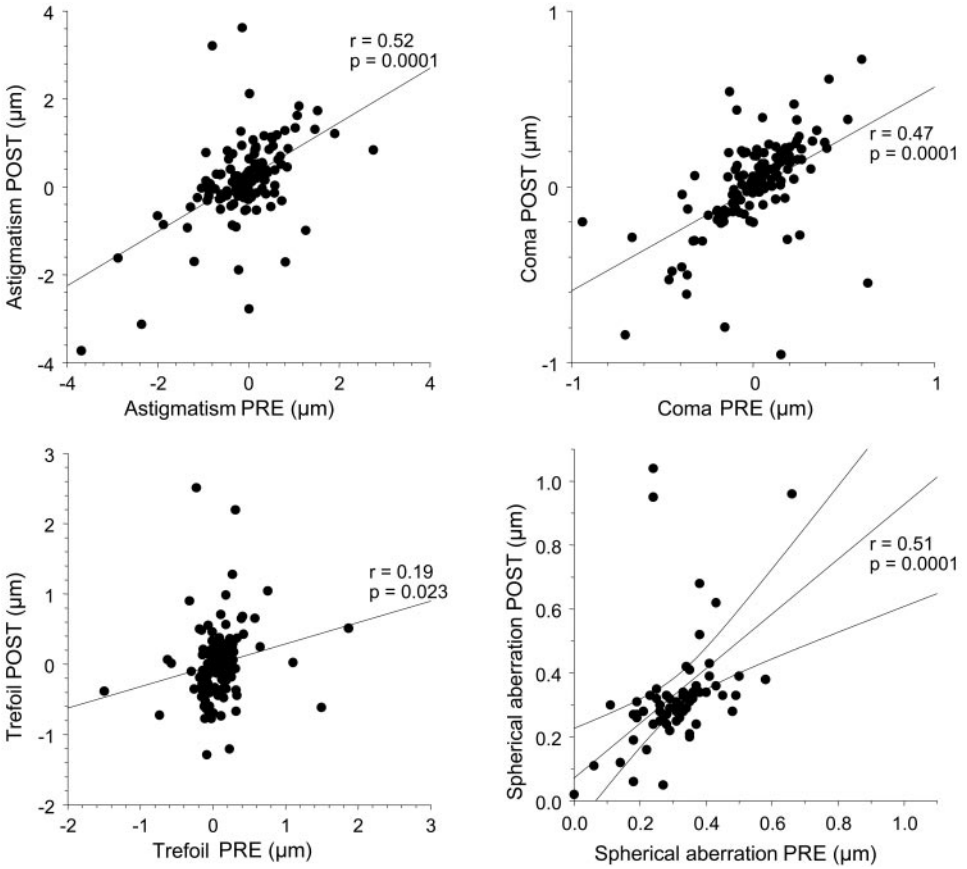

FIGURE 4. Zernike coefficients for corneal astigmatism ($c_2^{\pm 2}$), coma ($c_3^{\pm 1}$), trefoil ($c_3^{\pm 3}$), and spherical aberration (c_4^0), before and after surgery in each patient.

$$\Delta c_n^m = c_n^m(post) - c_n^m(pre). \quad (6)$$

In particular, we studied induced spherical aberration, astigmatism, coma, and trefoil. In the case of the nonrotationally symmetric aberrations (astigmatism, coma, and trefoil), we obtained both the magnitude and the orientation of the induced aberration. Thus, the induced astigmatism in polar values was calculated as

$$-\frac{4\sqrt{6}}{r_o^2}\sqrt{(\Delta c_2^{-2})^2 + (\Delta c_2^{+2})^2}\ \text{D};\ axis = \frac{1}{2}\arctan(\Delta c_2^{-2}/\Delta c_2^{+2})\ \text{degrees}. \quad (7)$$

The induced coma was calculated as

$$\sqrt{(\Delta c_3^{-1})^2 + (\Delta c_3^{+1})^2}\ \mu\text{m},\ axis = \arctan(\Delta c_3^{-1}/\Delta c_3^{+1})\ \text{degrees}, \quad (8)$$

and the induced trefoil as

$$\sqrt{(\Delta c_3^{-3})^2 + (\Delta c_3^{+3})^2}\ \mu\text{m},\ axis = \frac{1}{3}\arctan(\Delta c_3^{-3}/\Delta c_3^{+3})\ \text{degrees}. \quad (9)$$

RESULTS

Figure 3 shows the RMS, which indicates the total amount of higher order aberrations in every cornea before and after surgery. In most patients, the total amount of aberrations was similar before and after surgery. On average, the surgery did not systematically increase aberrations in the cornea, although it induced individual changes. The subgroup of patients with nasal incisions had a change of 0.3 ± 0.8 μm in the RMS, whereas the subgroup with temporal incisions had a change of 0 ± 0.5 μm. The postoperative corneal aberrations were much larger in a few patients (Fig 3, points labeled a–d), who had a nasal incision. In these corneas, the surgery produced a large increase in all aberrations and, in particular, induced a large horizontal astigmatism. In contrast, a few patients who had large preoperative corneal aberrations (Fig. 3, points labeled e, f), experienced a reduction. Patient e (nasal incision) had a large amount of trefoil at 0° that was reduced by the surgery. Patient f (temporal incision) had a large astigmatism.

Table 1 shows the mean ± SD of the aberrations averaged across all patients and the statistical comparison between the pre- and postoperative samples. The magnitude of the aberrations was similar to that previously found in normal corneas.[22] Both the paired *t*-test and the Wilcoxon test indicated that mean coma, and spherical aberration were statistically equal ($P > 0.05$: 95% confidence interval) in the two samples, whereas overall aberrations (RMS), astigmatism and trefoil were significantly different (on average, slightly higher in the postsurgical cornea) between the pre- and postsurgical samples. It must be noted that the statistical tests applied separately to the subgroups with nasal and temporal incisions

TABLE 2. Mean Induced Aberrations

Aberration	Mean Induced Value (Orientation)
Spherical aberration (μm)	0.03 ± 0.17
Astigmatism (D)	−1.00 ± 0.90 (predominant axis at the incision)
Coma (μm)	0.20 ± 0.30 (no predominant axis)
Trefoil (μm)	0.60 ± 0.60 (predominant axis at the incision)

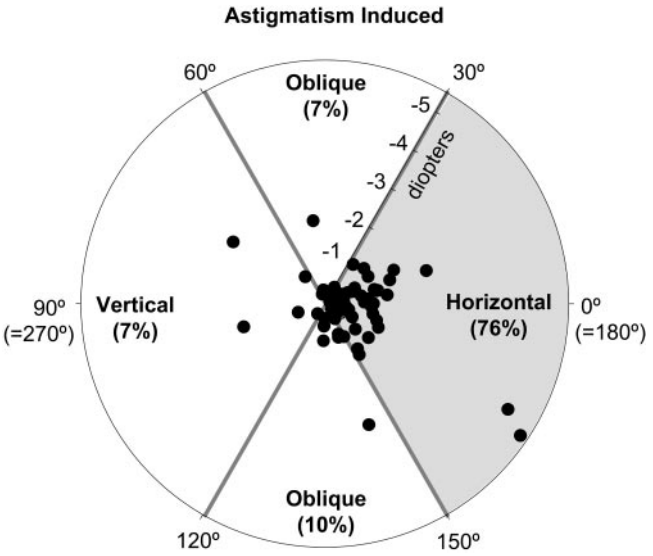

FIGURE 5. Astigmatism induced after surgery. The radial coordinate is the amount in diopters, and the angular coordinate is the axis scaled between 0° and 180°. The three regions group horizontal, oblique, and vertical astigmatisms. The *numbers* indicate the percentage of patients within each group. The *shaded area* indicates the dominant pattern (horizontal) of the induced astigmatism.

yielded an RMS in patients with temporal incisions that did not change significantly, whereas the RMS in patients with nasal incisions changed. This indicates that the slight increase of the RMS is mainly due to the changes in patients with nasal incisions.

The plots in Figure 4 show the Zernike coefficients for corneal astigmatism ($c_2^{\pm 2}$), coma ($c_3^{\pm 1}$), trefoil ($c_3^{\pm 3}$), and spherical aberration (c_4^0), before and after surgery in every patient. The correlations between aberrations before and after surgery are statistically significant, except for trefoil. On average, the amount of each aberration was similar before and after surgery. However, there were many individual variations, with some patients experiencing a slight reduction and others an increase. The plot for spherical aberration includes the 99% confidence interval, indicating the region where one can expect to find the 99% of the cases. The induced spherical aberration is 0.03 ± 0.17 μm on average (Table 2), and it may be positive or negative. The ratio between the induced spherical aberration and its preoperative value was calculated as a measure of the relative change induced by surgery. Thirty percent of the patients had a relative change lower than 10% and 50% had a relative change lower than 20%.

The astigmatism induced after surgery is shown in Figure 5. The radial coordinate in the polar plot indicates the amount in diopters, and the angular coordinate indicates the axis (meridian with the lowest curvature). Because α and α + 180° correspond to the same axis, the plot was scaled between 0° and 180°. Three regions have been delineated in the plot to classify horizontal, oblique, and vertical astigmatisms. Each of these groups covers the same area in the angle space. In most corneas, the surgery induced horizontal astigmatism. Seventy-six percent of the cases were between −30° (150°) and 30° (210°). Note that the probability of having the axis in the interval −30°, 30° by chance is only 33%. These results indicate that there was a dominant pattern of astigmatism induced by surgery, horizontal in our study, that was determined by the position of the incision (see Fig. 1). The mean value of the induced astigmatism was approximately −1 D. The induced aberration did not necessarily imply an increase in aberrations. Depending on the preoperative aberrations, there was an increase, no change, or even a decrease.

Figure 6 represents the magnitude and direction of the coma induced by the surgery. The axis was distributed with the same frequency in all directions. In this case, there was no orientation pattern. The amount of the coma induced was 0.23 ± 0.30 μm on average.

Figure 7 plots the induced trefoil. The axis goes from 0° to 120° because of the symmetry of this aberration, which has three lobules spaced at 120°. In other words: α, α + 120°, and α + 240° correspond to the same axis for trefoil. Similarly, in Figure 7 we divided the total axis space into three regions of the same size. There was a significant pattern of trefoil, shown by the shaded area. Sixty-eight percent of the cases were in the interval (40°, 80°) ([160°, 200°] or [280°, 320°]), whereas the

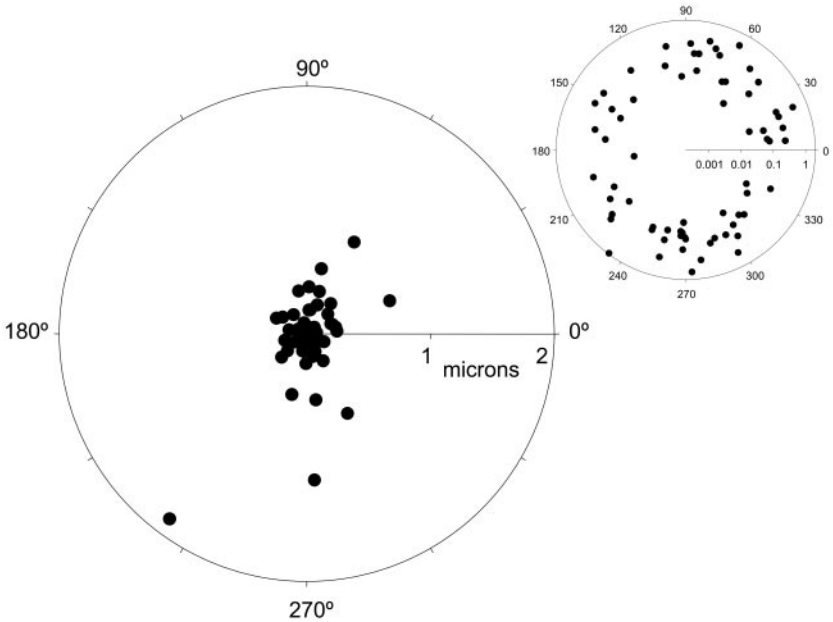

FIGURE 6. Magnitude and direction of coma induced by surgery. *Inset*: the magnitude in logarithmic scale.

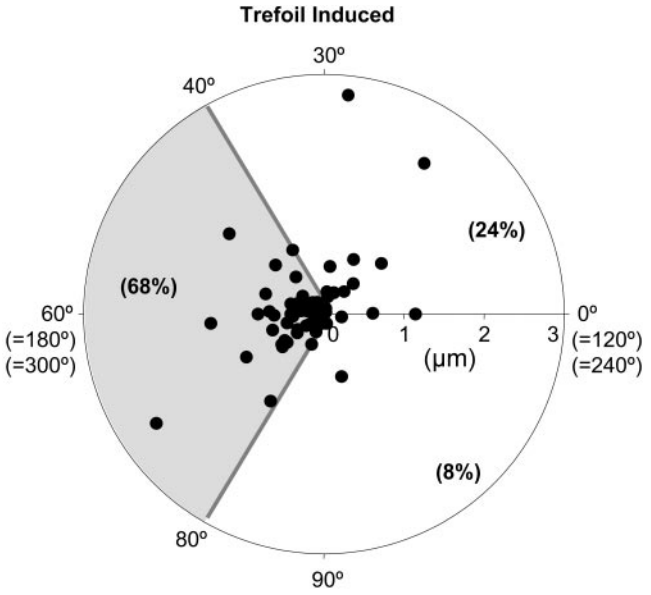

FIGURE 7. Magnitude and direction of the trefoil induced by surgery. The axis goes from 0° to 120°. The axis space is divided into three equal regions. The *numbers* are the percentage of patients within each region. The *shaded area* indicates the dominant pattern.

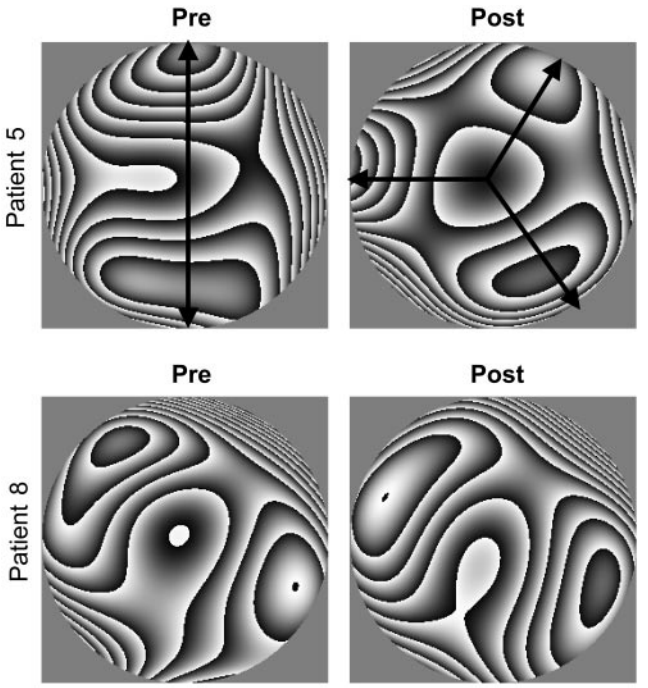

FIGURE 8. Wave aberration maps before and after surgery for two typical patients. The more steps the larger the amount of aberration. Aberrations are represented in modulus-π.

probability for a random distribution is 33%. The amount of trefoil induced was 0.57 ± 0.55 μm on average.

Figure 8 shows wave aberration maps before and after surgery in two patients who represent typical cases in the population. In patient 5, the surgery induced a horizontal astigmatism in the cornea that compensated for the preoperative corneal astigmatism and also induced a trefoil aberration at 180°. In the postoperative map the vertical astigmatism was reduced, and a structure with three lobules appeared instead. The second case (patient 8) was an example of almost no change in corneal optics after surgery. Figure 9 depicts the mean wave aberration in all eyes. These maps show a larger amount of aberration in the postoperative average eye than in the preoperative average eye. The map corresponding to the induced wave aberration indicates the mean change in the aberration profile after surgery. The dominant pattern in the induced aberration is horizontal astigmatism and trefoil oriented at 60°-180°-300°.

The histograms of Figure 10 indicate the percentage of patients whose corneas experience an induced astigmatism (and trefoil) at each orientation. As mentioned, the predominant orientation is 180° for both aberrations, which suggests that this is determined by the position of the incision. We propose a model considering that the probability of having an induced aberration (astigmatism or trefoil) oriented at an angle θ follows a Gaussian distribution

$$p(\theta) = \frac{1}{\sqrt{2}\sigma} \exp(-(\theta - \theta_i)^2/2\sigma^2), \qquad (10)$$

where we chose a width $\sigma = 17°$ (approximately half the angle subtended by the 3.5-mm incision at the limbus) and where θ_i is the position of the incision. Thus, we can estimate the percentage of subjects with an induced corneal aberration at θ by adding the probabilities of all patients

$$\sum_i p_i(\theta). \qquad (11)$$

The resultant function in equations 10 and 11 is plotted in Figure 10 as the solid line. The simulation describes reasonably well the experimental histograms. In particular, the model explains the skewed shape of the histograms slightly biased toward the third quadrant. This is because there were several patients with the incision within the third quadrant but no patient with the incision within the second quadrant.

DISCUSSION

Mean corneal aberrations were similar in degree or slightly larger after surgery than before surgery. This is in agreement with a study in which the corneal aberrations were compared in patients with rigid IOLs implanted after extracapsular cataract extraction (8- to 9-mm incision) with the aberrations in a group of normal subjects of similar age.[14] The results of the present work, obtained in the same patients before and after surgery, indicate that small 3.5-mm incision surgery produces only moderate changes and, on average, a small increase in aberrations. The larger changes occurred in the corneas with nasal incisions. However, the increase was not systematic. There were patients with almost no change and even some patients with a decrease in aberrations. Therefore, one can

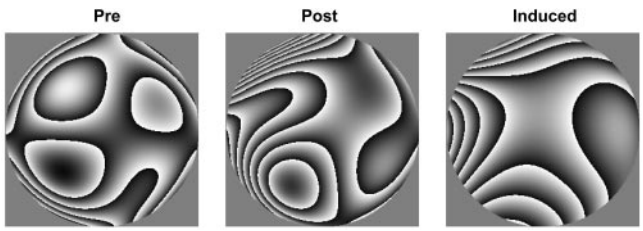

FIGURE 9. Maps showing the mean wave aberration in all eyes, for the preoperative, the postoperative, and the induced wave aberrations.

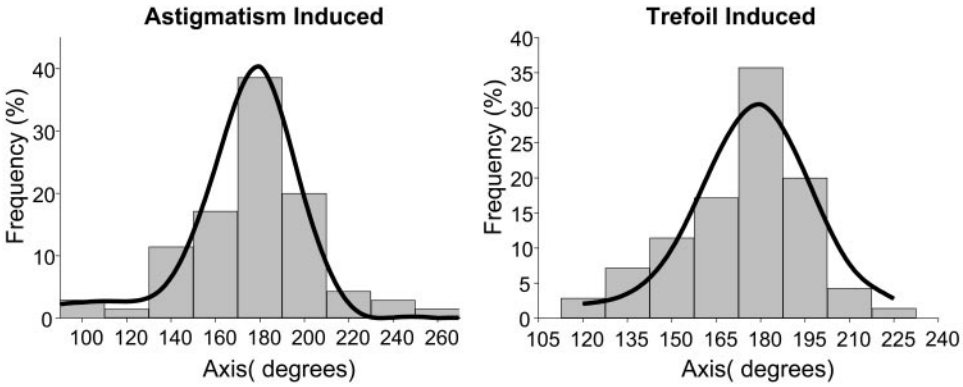

FIGURE 10. Percentage of patients whose corneas showed induced astigmatism (and trefoil) at each orientation. *Solid curves*: simulation according to the Gaussian model described in equation 10.

conclude that cataract surgery does systematically degrade the optical quality of the cornea, although it induces individual changes.

When the aberrations were analyzed in each patient, we found reasonable correlations between the aberration coefficients before and after surgery. However, there was a large dispersion, indicating that the surgery induced changes in the pattern of aberrations. The lowest changes occurred in spherical aberration. This seems to support the new concept of aspherical IOL designs for correcting the spherical aberration of the cornea, because this aberration does not change dramatically after surgery. A caveat regarding this approach is that the performance of such lenses rests on accurate positioning, centration, and stability after the implantation. With respect to other aberrations such as coma and trefoil, our results indicate that it would be ineffective to correct them with an IOL, because the expected change after surgery may be of the same magnitude as the original aberration. However, our results support the idea of a fully customized IOL with an aberration profile that could be controlled after implantation. With respect to this subject, it must be noted that aberrations with high angular order (for example, trefoil) do not have the same impact on visual performance as aberrations with low angular order or as rotationally symmetric aberrations.[23]

It seems that the position of the incision determines a predominant pattern of induced astigmatism and trefoil. The average pattern for induced astigmatism was 1 D in magnitude, with the axis of lowest curvature along the meridian of the incision, perhaps due to a biomechanical effect that may flatten the surgical meridian after wound healing. Similar results of surgically induced astigmatism with small incisions have been reported. For example, Beltrame et al.[11] found in 60 eyes with 3.5-mm incisions a mean induced astigmatism of 0.7 D. Steinert et al.[12] found an induced astigmatism of approximately 1 D with 4-mm incisions, and Naeser et al.[13] an astigmatism of 0.6 D averaged across 59 eyes, also with 4-mm incisions. The literature also supports the notion that the incisions may create a flattening of the surgical meridian. Kohnen et al.[24] reported a statistically significant difference in surgically induced corneal astigmatism after temporal and nasal unsutured limbal tunnel incisions. Recently, Barequet et al.[25] investigated in 178 eyes the astigmatism outcomes of temporal versus nasal clear corneal 3.5-mm incisions and found a shift toward with-the-rule astigmatism after surgery, which is affected by the side of the incision. On average, they measured a mean induced astigmatism of approximately 1 D at 6 weeks and 12 months. However, temporal incisions yielded a mean of 0.7 D and nasal incisions a mean of 1.5 D. This is in agreement with our results that temporal incisions induce less aberration than nasal incisions. We found that, in addition to astigmatism, the most significant changes in the overall aberrations occurred in the subgroup of patients who had nasal incisions. Our results and our model of the expected pattern could help to establish better criteria for selecting the incision site.

References

1. Liang J, Grimm B, Goelz S, Bille JF. Objective measurement of the WA's aberration of the human eye with the use of a Hartmann-Shack sensor. *J Opt Soc Am A*. 1994;11:1949–1957.
2. Prieto PM, Vargas-Martín F, Goelz S, Artal P. Analysis of the performance of the Hartmann-Shack sensor in the human eye. *J Opt Soc Am A*. 2000;17:1388–1398.
3. Iglesias I, Berrio E, Artal P. Estimates of the ocular wave aberration from pairs of double-pass retinal images. *J Opt Soc Am A*. 1998; 15:2466–2476.
4. He JC, Marcos S, Webb RH, Burns SA. Measurement of the wavefront aberration of the eye by a fast psychophysical procedure. *J Opt Soc Am A*. 1998;15:2449–2456.
5. Guirao A, Artal P. Corneal wave aberrations from videokeratography: accuracy and limitations of the procedure. *J Opt Soc Am A*. 2000;17:955–965.
6. Artal P, Guirao A. Contributions of the cornea and lens to the aberrations of the human eye. *Opt Lett*. 1998;23:1713–1715.
7. Artal, P, Guirao A, Berrio E, Williams DR. Compensation of corneal aberrations by the internal optics in the human eye. *J Vision* 2001;1:1–8. http://journalofvision.org/1/1/1, DOI 10.1167/1.1.1.
8. Artal P, Berrio E, Guirao A, Piers P. Contribution of the cornea and internal surfaces to the change of ocular aberrations with age. *J Opt Soc Am A*. 2002;19:137–143.
9. Mafra CH, Dave AS, Pilai CT, et al. Prospective study of corneal topographic changes produced by extracapsular cataract surgery. *Cornea*. 1996;15:196–203.
10. Chipont-Benabent E, Artola Roig A, Perez-Santonja JJ, et al. Astigmatism induced by intrastromal corneal suture after small incision phacoemulsification. *J Cataract Refract Surg*. 1998;24:519–523.
11. Beltrame G, Salvetat ML, Chizzolini M, Driussi G. Corneal topographic changes induced by different oblique cataract incisions. *J Cataract Refract Surg*. 2001;27:720–727.
12. Steinert RF, Brint SF, White SM, Fine IH. Astigmatism after small incision cataract surgery: a prospective, randomized, multicenter comparison of 4- and 6.5-mm incisions. *Ophthalmology*. 1991;98: 417–423.
13. Naeser K, Knudse EB, Hansen MK. Bivariate polar value analysis of surgically induced astigmatism. *J Refract Surg*. 2002;18:72–78.
14. Guirao A, Redondo M, Geraghty E, Piers P, Norrby S, Artal P. Corneal optical aberrations and retinal image quality in patients in whom monofocal intraocular lenses were implanted. *Arch Ophthalmol*. 2002;120:1143–1151.
15. Optical Laboratories Association. *American National Standard for Ophthalmics-Intraocular Lenses.* Merrifield VA: Optical Laboratories Association; 1994.
16. International Organization for Standardization. Ophthalmic implants—intraocular lenses. Part 2: optical properties and test meth-

ods. Geneva, Switzerland: International Organization for Standardization; 1999. Publication ISO 11979-2.

17. Simpson MJ. Optical quality of intraocular lenses. *J Cataract Refract Surg*. 1992;18:86–94.
18. Norrby NES. Standarized methods for assessing the imaging quality of intraocular lenses. *Appl Opt*. 1995;34:7327–7333.
19. Artal P, Marcos S, Navarro R, Miranda I, Ferro M. Through focus image quality of eyes implanted with monofocal and multifocal intraocular lenses. *Optical Eng*. 1995;34:772–779.
20. Schultze RL. Accuracy of corneal elevation with four corneal topography systems. *J Refract Surg*. 1998;14:100–104.
21. Guirao A, Williams DR. A method to predict refractive errors from wave aberration data. *Optom Vis Sci*. 2003;80:36–42.
22. Guirao A, Redondo M, Artal P. Optical aberrations of the human cornea as a function of age. *J Opt Soc Am A*. 2000;17:1697–1702.
23. Applegate RA, Ballentine C, Gross H, Sarver EJ, Sarver CA. Visual acuity as a function of Zernike mode and level of root mean square error. *Optom Vision Sci*. 2003;80:97–105.
24. Kohnen S, Neuber R, Kohnen T. Effect of temporal and nasal unsutured limbal tunnel incisions on induced astigmatism after phacoemulsification. *J Cataract Refract Surg*. 2002;28:821–825.
25. Barequet IS, Yu E, Vitale S, Cassard S, Azar DT, Stark WJ. Astigmatism outcomes of horizontal temporal versus nasal clear corneal incision cataract surgery. *J Cataract Refract Surg*. 2004;30:418–423.